Published online 18 August 2017 *Nucleic Acids Research, 2017, Vol. 45, No. 17* ***10321–10331***
doi: 10.1093/nar/gkx713

Influence of nucleotide modifications at the C2' position on the Hoogsteen base-paired parallel-stranded duplex of poly(A) RNA

William Copp[1,2,†], Alexey Y. Denisov[1,2,†], Jingwei Xie[2,3], Anne M. Noronha[1,2], Christopher Liczner[1,2], Nozhat Safaee[2,3], Christopher J. Wilds[1,2,*] and Kalle Gehring[2,3,*]

[1]Department of Chemistry and Biochemistry, Concordia University, Montréal, Québec H4B 1R6, Canada, [2]Groupe de recherché axé sur la structure des protéines, Montréal, Québec H3G 0B1, Canada and [3]Department of Biochemistry, McGill University, Montréal, Québec H3G 0B1, Canada

Received July 10, 2017; Revised July 29, 2017; Editorial Decision August 02, 2017; Accepted August 17, 2017

ABSTRACT

Polyadenylate (poly(A)) has the ability to form a parallel duplex with Hoogsteen adenine:adenine base pairs at low pH or in the presence of ammonium ions. In order to evaluate the potential of this structural motif for nucleic acid-based nanodevices, we characterized the effects on duplex stability of substitutions of the ribose sugar with 2′-deoxyribose, 2′-*O*-methyl-ribose, 2′-deoxy-2′-fluoro-ribose, arabinose and 2′-deoxy-2′-fluoro-arabinose. Deoxyribose substitutions destabilized the poly(A) duplex both at low pH and in the presence of ammonium ions: no duplex formation could be detected with poly(A) DNA oligomers. Other sugar C2' modifications gave a variety of effects. Arabinose and 2′-deoxy-2′-fluoro-arabinose nucleotides strongly destabilized poly(A) duplex formation. In contrast, 2′-*O*-methyl and 2′-deoxy-2′-fluoro-ribo modifications were stabilizing either at pH 4 or in the presence of ammonium ions. The differential effect suggests they could be used to design molecules selectively responsive to pH or ammonium ions. To understand the destabilization by deoxyribose, we determined the structures of poly(A) duplexes with a single DNA residue by nuclear magnetic resonance spectroscopy and X-ray crystallography. The structures revealed minor structural perturbations suggesting that the combination of sugar pucker propensity, hydrogen bonding, pKa shifts and changes in hydration determine duplex stability.

INTRODUCTION

Nucleic acids are attractive materials for nanotechnology as their structure and abilities for molecular recognition offer a range of applications, which include molecular switches, nanosensors, vehicles for drug delivery and gene silencing. RNA, a central participant in the regulation of gene expression, is gaining recognition as a nanomaterial due to its capacity to engage in non-canonical base pairing and adopt diverse, functional structures in response to environmental conditions (1).

In 2013, we determined the 1 Å X-ray crystal structure of a right-handed parallel-stranded duplex stabilized by adenine:adenine base pairing (2). The duplex was first identified by Rich and coworkers in 1961 from thermal denaturation and X-ray fibre diffraction data (3). The base-pairing motif involves the Hoogsteen faces of the adenine bases with the exocyclic amine group hydrogen bonding with the N7 ring atom and phosphate of the opposing strand (Figure 1A). This motif has 180° rotational symmetry which leads to a parallel-stranded duplex (4).

The adenine:adenine base pairing is stabilized by either low pH or ammonium (NH_4^+) ions. Rich and coworkers proposed that, under acidic conditions, protonation of the N1 atom of adenine occurs. The positive charge is positioned to interact electrostatically with the negatively charged phosphate of the opposing strand and stabilizes duplex formation. Our 1 Å X-ray crystal structure of the parallel duplex was determined with crystals grown in the presence of NH_4^+ cations at pH 7.2. Based on measurement of bond angles of the adenine bases, we showed that the adenine rings were not protonated in the crystal. Instead, bound NH_4^+ ions were positioned to interact with the unprotonated N1 atom of adenine and a non-bridging oxygen atom of a phosphate group of the nucleotide engaged in the adenine:adenine base pairing on the opposing strand.

*To whom correspondence should be addressed. Kalle Gehring. Tel: +1 514 398 7287; Fax: +1 514 398 7384; Email: Kalle.Gehring@mcgill.ca
Correspondence may also be addressed to Christopher J. Wilds. Tel: +1 514 848 2424 (Ext. 5798); Fax: +1 514 848 2868; Email: Chris.Wilds@concordia.ca
†These authors contributed equally to the paper as first authors.

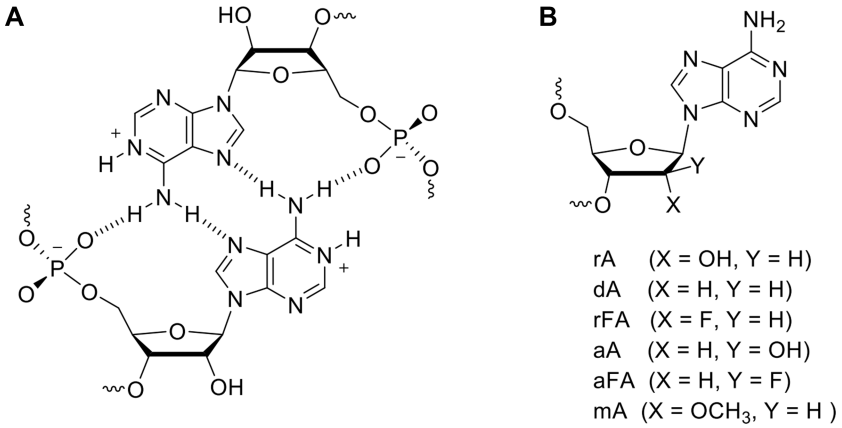

Figure 1. (**A**) Adenine base pairing with protonation at N1 and (**B**) 2′-modifications evaluated in this study.

Recently, Maquat and co-workers solved the X-ray crystal structure of a duplex of rA_7 formed at pH 3.5 in the presence of NH_4^+ cations (5). This structure is composed of alternating protonated and unprotonated adenine bases where an NH_4^+ ion is bound to every other adenine:adenine base pair.

Nucleic acids can adopt numerous other parallel-stranded structures (6–9). An early work by Jovin *et al.* reported a parallel-stranded duplex stabilized by 'reverse Watson–Crick' A:T base pairing; however, it shows reduced thermal stability relative to its antiparallel-stranded counterpart (7). Another well-studied parallel-stranded DNA structure is the i-motif which consists of intercalated parallel-stranded duplexes and forms under acidic conditions (10). Recently, a parallel-stranded duplex was engineered consisting of non-natural isoguanine and 5-methylcytosine nucleobases, further adding to the growing repertoire of parallel-stranded duplexes (11). The majority of parallel-stranded structures described have been formed with DNA.

Modification of the scaffold of nucleic acids, achieved through solid-phase chemical synthesis, can enhance their properties (12,13). This has led to the design of analogs that demonstrate improved stability and resistance to enzymatic degradation as antisense and RNAi-based therapeutics. The influence of chemical modification to the nucleic acid backbone has been investigated for various structures including the i-motif where substitution with cytidine (RNA) was found to decrease the thermal stability of this structure (14). Recently, Damha reported that the i-motif structure can form at a pH of 7 when the DNA sugars are replaced by 2′-deoxy-2′-fluoro-arabinose (15).

Here, we acquired the first nuclear magnetic resonance (NMR) spectra of a parallel poly(A) duplex and characterized its solution structure at pH 4. We investigated the influence of modifications at the C2' position of the sugar moiety of the nucleotide on formation of the poly(A) duplex. Poly(A) oligonucleotides were prepared where adenosine was replaced by 2′-deoxyadenosine (dA), 2′-deoxy-2′-fluoro-riboadenosine (rFA), 2′-O-methyl-riboadenosine (mA), arabinoadenosine (aA) and 2′-deoxy-2′-fluoro-arabinoadenosine (aFA). The influence of these modifications on the thermal stability of the poly(A) duplex was examined by ultraviolet (UV) thermal denaturation experiments and the structure of a single dA residue in a parallel duplex was evaluated by NMR spectroscopy and X-ray crystallography. Understanding the effects of sugar modifications on the poly(A) duplex is important for the design of nucleic acid structures with novel functionalities for nanoscience.

MATERIALS AND METHODS

Oligonucleotide synthesis, purification and characterization

All phosphoramidites and ancillary reagents were obtained from Glen Research (Sterling, Virginia). All oligonucleotides were synthesized on 1 μmol scale with an Applied Biosystems Model 3400 synthesizer using standard β-cyanoethylphosphoramidite chemistry with long chain alkylamine controlled pore glass (LCAA-CPG) used as the solid support. The synthesis protocol was supplied by the manufacturer with only minor modifications made to the coupling times. Cleavage of the oligonucleotides from the CPG and removal of the protecting groups was achieved with 1 ml NH_4OH (aqueous, 28%): ethanol (3:1) for a minimum of 4 h at 55°C (16). For oligonucleotides containing rA an additional deprotection step was performed consisting of incubation at 65°C with 200 μl of TEA·3HF for a minimum of 2 h to remove the 2′-O-TBDMS group. The crude oligonucleotides were precipitated from 400 μl of anhydrous methanol and washed twice with 400 μl of anhydrous methanol to remove all residual TEA·3HF. Oligonucleotides were purified by preparatory denaturing polyacrylamide gel electrophoresis (PAGE) or ion-exchange (IEX) high performance liquid chromatography (HPLC). The preparatory denaturing PAGE consisted of a 20% acrylamide solution (19:1 acrylamide:bisacrylamide) in 1 × Tris/Borate/EDTA (TBE) running buffer on standard 20 × 20 cm glass plates at 450 V until sufficient separation was achieved. The desired band was excised and the pure oligonucleotide was extracted with 8–10 ml of 0.1 M NaOAc (sodium acetate) solution on a mixer overnight. Purification by IEX-HPLC was performed using a Dionex DNAPAC PA-100 column (0.4 × 25 cm) with a linear gradient of 0–50% buffer B over 30 min (buffer A: 100 mM Tris–HCl, pH 7.5, 10% acetonitrile (ACN) and buffer B: 100

mM Tris–HCl, pH 7.5, 10% ACN, 1 M NaCl). The collected fraction was diluted by $\frac{1}{4}$ with 0.1 M NaOAc and desalted with a C-18 SEP PAK cartridge. The cartridge was prepared by washing with 10 ml of HPLC grade ACN, followed by 50% ACN and finally equilibrated with 0.1 M NaOAc. The oligonucleotide was adsorbed to the C-18 column then the salt was removed with 2 × 10 ml of water. The sample was eluted with methanol:water:ACN (2:1:1) eluent. Purity was assessed to be >90% for all oligonucleotides synthesized by analytical denaturing PAGE or IEX HPLC. All oligonucleotides were quantitated using a Varian Cary Model 3E spectrophotometer. Single strand concentrations were calculated using the Beer–Lambert law and the absorbance was measured at 260 nm. Molar extinction coefficients were calculated by the nearest neighbor approximation (17). The extinction coefficient for 2′ modified nucleotides was assumed to be identical to the unmodified sequence. The purity and identity of oligonucleotides was assessed by mass spectrometry at the Concordia University Centre for Biological Applications of Mass Spectrometry (Supplementary Table S1). 0.1 OD of oligonucleotide was dried down for ESI-qTOF MS analysis on a Micromass qTOF Ultima API. The mass spectrometer was run in full scan, negative ion detection mode.

UV thermal denaturation studies

Oligonucleotides were suspended in 1 ml of buffer, heated at 95°C for 10 min, slowly cooled to room temperature and incubated at 4°C overnight. The samples were then degassed on the speed-vacuum concentrator for 2 min. UV thermal denaturation data were acquired with a Varian CARY Model 3E Spectrophotometer Varian fitted with a 12-sample thermostated cell block and a temperature controller, with absorbance measured at 260 nm and a heating rate of 0.5°C/min. The melting temperature (T_m) was calculated as the maximum of the first derivative according to the method of Puglisi and Tinoco (17). All data analysis were performed with Microsoft Excel™.

Native polyacrylamide gel electrophoresis

The oligonucleotide of 0.1 OD was suspended in 10 μl of phosphate-citrate (40 mM Na_2HPO_4, 30 mM citric acid and pH 4 or pH 7) sucrose loading buffer. The samples were heated at 95°C for 10 min, slowly cooled to room temperature and incubated at 4°C for 1 h. Gels were prepared with 50% acrylamide/bisacrylamide (40% acrylamide, 19:1):50% running buffer (40 mM Na_2HPO_4, 30 mM citric acid and pH 4 or pH 7). Gels were polymerized between two 7 × 10 cm glass plates and were prerun for 20 min at 80 V in a temperature-controlled apparatus at 10°C.

NMR spectroscopy experiments

One millimolar solution of duplex was prepared with an oligonucleotide composed of the sequence 5′-dT-mA_4-dA-mA_3 (where dT is thymidine, dA is 2′-deoxyadenosine and mA is 2′-O-methyladenosine) by dissolving the sample in 400 μl of 100% D_2O or 90% H_2O/10% D_2O buffer containing 50 mM Na-acetate-d_3. The pH was adjusted to 4 by the addition of 0.1 M HCl. Proton NMR spectra were recorded on Bruker and Varian 800, 600 and 500 MHz spectrometers equipped with cryoprobes. NOESY experiments were performed in D_2O at 10°C using mixing times of 70 and 250 ms. DQF-COSY spectra were collected without phosphorus decoupling. Proton TOCSY MLEV-16 experiments were performed with a mixing time of 75 ms. NOESY experiments for imino-protons in 9:1 H_2O/D_2O were performed at 10°C with mixing times of 70 and 200 ms. Phosphorus spectra and H,P-correlation HSQC spectra (with $J_{PH} = 30$ Hz) were recorded on a Varian VNMRS (^{31}P NMR 202 MHz and ^{1}H NMR 500 MHz) at 25°C. All spectra were processed by NMRPipe (18). NOESY cross-peak volumes were calculated using NMRView (19). Phosphorus resonances were indirectly referenced to 85% H_3PO_4 (20).

Structural modeling and molecular dynamics

Distance restraints were derived from the NOESY spectra at different mixing times by integrating the cross-peak volumes, scaled using the d^{-6} distance relationship and average cross-peak volume values for calibration by the methyl-H6 distance in thymidine (d = 2.70 Å). The distance constraints were input in the software with 10% lower and 15% upper bounds. The five torsion angles for the sugars were constrained to the N-type range (C3'-*endo*). The β-torsion angles were constrained using the information from the H5'/H5'-P and H4'-P cross-peaks in the H,P-HSQC spectra. The β angles were found to reside in the trans conformation (180 ± 30°) as determined by the relatively low intensity of the H5'/H5'-P cross-peaks as well as moderate ^{4}J(H4'-P) W-pathway couplings. The γ angles were constrained (60 ± 20°) using the Nuclear Overhauser Spectroscopy (NOESY) H4'-H1' cross-peak linewidths (∼17 Hz) and the ^{4}J(H4'-P) W-pathway couplings (21). Phosphorus chemical shifts were found to span a very narrow region and the ϵ angles have been constrained from the strong intensity H3'-P cross-peaks (220 ± 40°). Finally, the glycosidic angles (χ) were not constrained in structure calculations but were fixed indirectly by intra-nucleotide aromatic-sugar distances.

The starting coordinates of the 2′-deoxyadenosine and 2′-O-methyladenosine portion of the duplex formed by dT-mA_4-dA-mA_3 were generated from the structure (PDB ID: 4JRD) of a poly(A) duplex (2). CNS 1.2 software with a nucleic acid all-hydrogen force field was used for molecular modeling (22). The calculation was based on 150 NOE-distances, 124 torsion angles and 30 hydrogen bond restraints. Gentle refinement was accomplished by molecular dynamics simulation (15 ps at 2000 K, then slow-cool annealing to 0 K) including a Cartesian cooling stage. The ten best structures were collected and global helical parameters were calculated using the 3DNA 2.1 program (23,24).

Crystallization, structure determination and refinement

Crystals were obtained by the hanging drop method by equilibrating 0.5 μl of a 1:1 complex of 5′-rA_5-dA-rA_5 and the RRM23 fragment (residues 98–269) of poly(A) binding protein in buffer (10 mM HEPES, 100 mM NaCl, 2 mM dithiothreitol (DTT) and pH 7.0) with 0.5 μl of 1.6 M $(NH_4)_2SO_4$, 0.1 M citric acid and pH 5 at 22°C. Data

were collected from crystals in cryoprotectant solution on a MarMosaic CCD 300 detector at beamline 08ID-1 at the Canadian Light Source (Saskatoon, Canada). The structure was solved by molecular replacement using the $(rA)_{11}$ duplex (PDB ID: 4JRD).

RESULTS

Deoxyribose destabilizes the poly(A) duplex

The influence of deoxyribose residues on the stability of the poly(A) RNA duplex was evaluated in two series of oligomers containing 9 and 16 residues. The 9-mer series, dT-rA_8, was composed of eight adenosines (rA) with a single thymidine (dT) at the 5′ end to introduce asymmetry in the sequence for NMR studies: a strategy used in studies of other homo-oligomers (10,25). UV thermal denaturation experiments revealed that dA substitutions destabilized dT-rA_8 duplex formed at pH 4 with a decrease in T_m of ∼8°C for each dA residue added (Table 1 and Figure 2A). For the 16-mer series, the dA substitutions had a smaller destabilizing influence with a decrease in the T_m of ∼3°C per dA residue (Table 1 and Figure 2B). The smaller destabilizing effect likely reflects the high degree of cooperativity in duplex formation where the T_m is principally determined by the length of the longest run of consecutive rA residues. For both 9-mer and 16-mer sequences, the fully substituted deoxyribose oligomers displayed a linear increase in absorbance previously ascribed to unstacking of adenine bases in the single strand (26). The absence of a sigmoidal transition strongly suggests the absence of duplex formation by the poly dA oligomers.

To examine the origin of destabilization from dA inserts, van't Hoff analysis was performed to estimate the enthalpic, entropic and Gibbs' free energy components of duplex formation. The melting temperature concentration dependence of the RNA 9mer, dT-rA_8, as well as those with one and two dA inserts was exploited to determine the van't Hoff thermodynamic parameters (Table 2). The data for the oligonucleotide containing three dA inserts were not included as the lack of lower plateau did not allow for an accurate determination of the melting temperature. The thermodynamic source of the destabilization appears to be entropic as there is a loss of entropy change as the dA content is increased. A potential explanation is loss of conformational preorganization of the single strands (27).

The influence of dA substitutions on poly(A) duplex formation was also evaluated at neutral pH in the presence of a high concentration of NH_4^+ (Table 1 and Figure 2C). Due to the decreased stability of the duplex in NH_4^+ relative to low pH, the denaturation experiments were conducted with longer, 16-mer oligomers. Analysis of sequences with one, two or three substitutions showed that each deoxyribose led to a decrease of ∼8°C in stability at pH 7 in the presence of 4.4 M NH_4Cl. Again, no thermal transition was observed for the all DNA oligomer. To confirm the absence of duplex formation by DNA oligomers, we employed three complementary techniques: gel electrophoresis, circular dichroism and NMR spectroscopy.

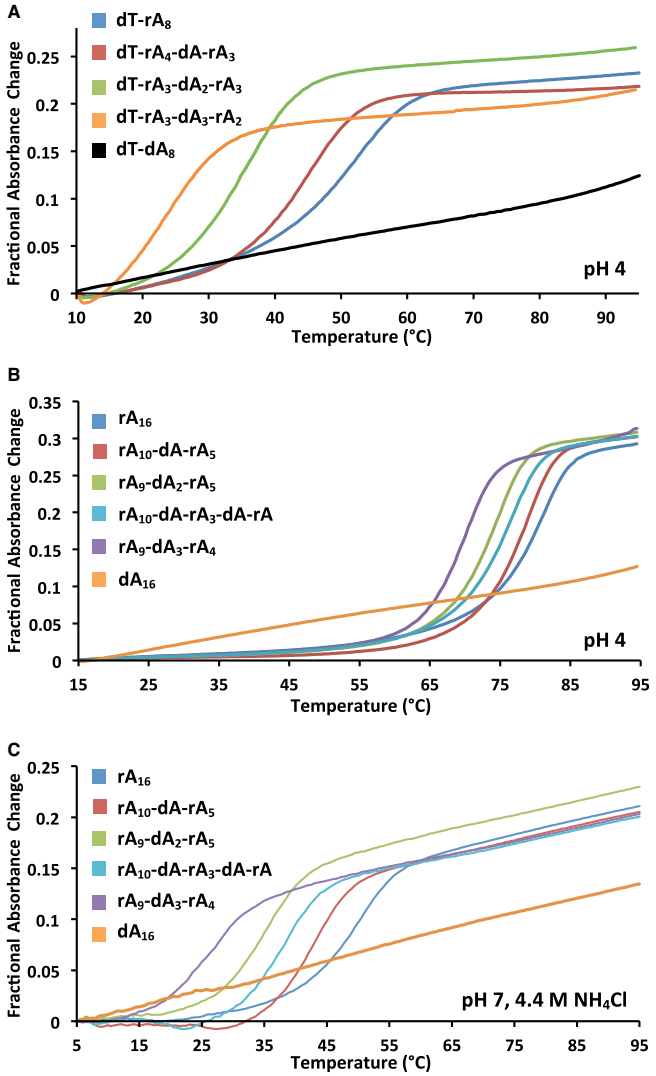

Figure 2. Deoxyribose residues destabilize the poly(A) duplex. UV thermal denaturation profiles of rA-dA chimera of (**A**) 9-mers and (**B**) 16-mers at pH 4 and (**C**) 16-mers in ammonium chloride solution. Buffer was 50 mM NaOAc at pH 4 and 40 mM Na_2HPO_4, 30 mM citric acid at pH 7. Strand concentrations were 4.2 μM for the 9-mers and 2.3 μM for the 16-mers.

Poly(A) DNA does not form a duplex at low pH

NMR spectroscopy confirmed duplex formation by poly(A) RNA at pH 4 (Figure 3A). To our knowledge, this is the first characterization of a parallel poly(A) duplex by NMR. We examined the oligomer dT-rA_8: the thymidylate is easily identified in the NMR spectrum and appears to promote alignment of the two strands. At pH 4, the NMR spectrum revealed well-resolved amino signals around 9 ppm, which are indicative of nucleic acid base pairing. NOESY and COSY spectra confirmed the NMR signal assignments and parallel duplex structure (Supplementary Table S2). The number of resonances in the RNA spectrum indicates that the two strands in the poly(A) RNA duplex are identical. In contrast, the NMR spectrum of the DNA oligomer dT-dA_8 showed no evidence of base pairing or duplex formation. The NOESY spectrum showed none of the char-

Table 1. Thermal melting temperatures of adenine oligonucleotides

	Sequence (5′–3′)	pH 4[a]		pH 7, 4.4 M NH_4Cl[b]	
		T_m	ΔT_m[c]	T_m	ΔT_m
Deoxyribo-nucleotides (dA)	**dT-r(AAAAAAAA)**	53	-		
	dT-r(AAAA)-dA-r(AAA)	45	-8		
	dT-r(AAA)-d(AA)-r(AAA)	37	-16		
	dT-r(AAA)-d(AAA)-r(AA)	<24	<–29		
	d(TAAAAAAAA)	NT[d]			
	r(AAAAAAAAAAAAAAAA)	82	-	51	-
	r(AAAAAAAAAA)-dA-r(AAAAA)	80	-2	42	-9
	r(AAAAAAAAA)-d(AA)-r(AAAAA)	75	-7	36	-15
	r(AAAAAAAAA)-dA-r(AAA)-dA-rA	77	-5	39	-12
	r(AAAAAAAAA)-d(AAA)-r(AAAA)	71	-11	28	-23
	d(AAAAAAAAAAAAAAAA)	NT		NT	
Fluororibo-nucleotides (rFA)	**r(AAAAAAAAAA)**	66	-		
	r(AAAAA)-rFA-r(AAAAA)	64	-2		
	r(AAAAA)-rF(AA)-r(AAAA)	61	-5		
	r(AAAA)-rF(AAA)-r(AAAA)	58	-8		
	rF(AAAAAAAAAA)	51	-15		
	dT-r(AAAA)-rFA-r(AAA)	52	-1		
	r(AAAAAAAAAA)-rFA-r(AAAAA)			52	+1
	rF(AAAAAAAAAAAAAAAA)			64	+13
Arabinonucleotides (aA)/ fluoroarabino-nucleotides (aFA)	dT-r(AAAA)-aA-r(AAA)	<25	<-28		
	dT-r(AAAA)-aFA-r(AAA)	<25	<-28		
	dT-a(AAAAAAAA)	NT			
	dT-aF(AAAAAAAA)	NT			
Methylribo-nucleotides (mA)	dT-r(AAAA)-mA-r(AAA)	57	+4		
	dT-m(AAAAAAAA)	63	+10		
	dT-m(AAAA)-dA-m(AAA)	55	+2		
	m(AAAAAAAAAAAAAAAA)			52	+1

[a]Buffer: 50 mM NaOAc, pH 4.
[b]Buffer: 4.4 M NH_4Cl, 40 mM Na_2HPO_4, 30 mM citric acid, pH 7.
[c]Difference in T_m compared to RNA sequence (in bold) in same buffer.
[d]NT: no transition detected.

Table 2. Thermodynamic parameters of duplex formation of oligoadenylates with dA residues

Sequence (5′–3′)	$\Delta H°$ (kJ mol^{-1})	$\Delta\Delta H°$	$\Delta S°$ (J K^{-1} mol^{-1})	$\Delta\Delta S°$	$\Delta G°$ (kJ mol^{-1}) at 25°C	T_m (°C) at 4 μM
dT-rA_8	−249±32		−665±87		−50.9	53
dT-rA_4-dA-rA_3	−293±44	44	−816±124	151	−49.3	45
dT-rA_3-dA_2-rA_3	−313±10	64	−904±30	239	−43.0	37

acteristic cross-peaks observed with the RNA sample (see below).

Large differences in the conformations of poly(A) RNA and DNA oligomers were also detected by circular dichroism and gel electrophoresis. The circular dichroism spectrum of dT-rA_8 at pH 4 showed a large peak at 260 nm and a small dip at 245 nm, as previously reported for poly(A) RNA (28). In contrast, the DNA oligomer dT-dA_8 showed much weaker overall ellipicity and different peak wavelengths (Figure 3B). Polyacrylamide gel electrophoresis showed a pH-dependent migration of the RNA oligomers rA_{11} and rA_{16}, indicative of the formation of a duplex at low pH (Figure 3C). At pH 4, the RNA oligomers migrated more slowly than control DNA oligomers rU_{11} and rU_{16} while the DNA oligomers, dA_{11} and dA_{16}, migrated identically with control dT_{11} and dT_{16} oligomers. At pH 7, both the rA and dA sequences migrated slightly faster than the control pyrimidine sequences, which may be due to partial structuring of the poly(A) single strands (26).

Influence of 2′-F-ribose, 2′-O-methyl-ribose and arabinose on the stability of the poly(A) duplex

Poly(A) oligomers containing different modifications at the C2' position were prepared to evaluate the influence of sugar modifications on duplex stability. UV thermal denaturation experiments of 11-mer oligomers with 2′-F-ribose substitutions showed a reduction in T_m of ∼2.5°C for each rFA residue at pH 4 (Table 1 and Supplementary Figure S1). The destabilization appeared to be pH dependent as the longer oligomers rA_{16} and rFA_{16} showed the essentially the same T_m at pH 3.5 (Supplementary Figure S2). At pH 5, rFA_{16} showed no sigmoidal transition whereas rA_{16} had a T_m of 39°C. Paradoxically, at neutral pH and 4.4 M NH_4Cl, rFA residues stabilized the duplex. A single rFA substitution in the 16-mer duplex provided a moderate increase in T_m of 1°C and the fully substituted oligomer rFA_{16} was significantly stabilized by 13°C (Supplementary Figure S3). It has been reported that the origin of the enhanced stability of antiparallel stranded duplexes formed by strands containing 2′-F-ribose compared to ribose is enthalpy driven

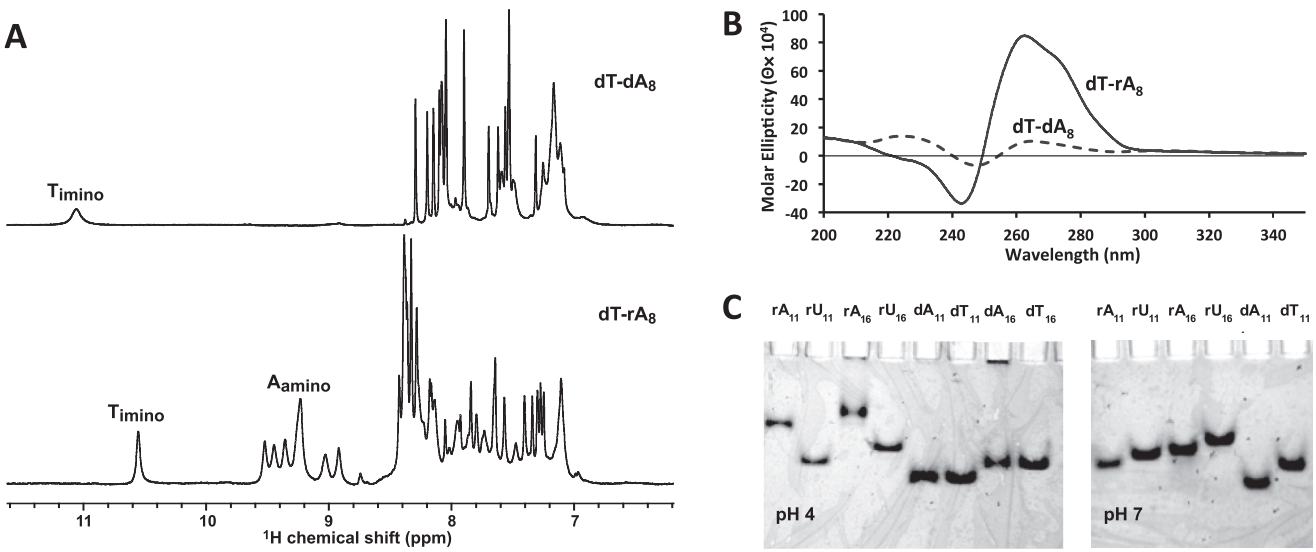

Figure 3. Absence of poly(A) duplex formation by DNA but not RNA oligomers. (**A**) Nuclear magnetic resonance (NMR) spectra of poly(A) RNA show amino signals indicative of adenine base pairing. Spectra were recorded at 600 MHz with jump-return excitation at pH 4, 2°C. (**B**) Circular dichroism spectra of poly(A) oligomers in 50 mM NaOAc, pH 4, at 20°C. (**C**) Native polyacrylamide gel electrophoresis at pH 4 and 7 shows pH-dependent migration shift of poly(A) RNA but not poly(A) DNA. The gels were 20% acrylamide:bisacrylamide (19:1) in 39 mM Na_2HPO_4, 31 mM citric acid, 1.1 mM ethylenediaminetetraacetic acid, run at 80 V for 3 h and visualized by UV shadowing.

due to strengthened hydrogen bonding and stacking interactions in the duplex (29).

UV melting curves showed that that 2′-O-methyl-ribose substitutions also stabilized the poly(A) duplex. A single mA substituted into the dT-rA_8 duplex increased the T_m by 4°C. The fully substituted duplex, dT-mA_8, was 10°C more stable than the corresponding RNA duplex (Table 1 and Supplementary Figure S4). This agrees with the early observation by Cerutti and coworkers that methylation of the 2′-hydroxy group of poly(A) led to an increase in the thermal stability of poly(A) duplexes (28). Surprisingly, we observed that the stabilization of duplex was limited to acidic conditions. Comparison of the melting temperatures of 16-mers at neutral pH and 4.4 M NH_4^+ ions showed only a small 1°C increase in duplex stability (Table 1 and Supplementary Figure S5). We also tested the effect of a deoxyribose sugar in the context of the methylated duplex. Again DNA nucleotides were destabilizing. Insertion of single deoxyribose decreased the T_m of the 2′-O-methylated duplex by ∼8°C. The largest effects on duplex stability were observed with substitutions of ribose by its 2′-epimer, arabinose or 2′-deoxy-2′-fluoro-arabinose. Both very strongly destabilized the duplex. UV thermal denaturation on the 9-mer dT-rA_8 series with single arabinose (aA) or 2′-fluoro-arabinsoe (aFA) measured a reduction in T_m of roughly 30°C at pH 4. No sigmoidal transitions were observed with the fully substituted aA or aFA oligonucleotides (Table 1 and Supplementary Figure S6). To our knowledge, this is the first example of destabilization of a duplex by 2′-deoxy-2′-fluoro-arabinose.

X-ray crystal structure of the rA_5-dA-rA_5 duplex

We turned to X-ray crystallography and NMR spectroscopy to understand the sensitivity of duplex stability to modifications of the C2’ position. Crystals of the duplex formed by rA_5-dA-rA_5 were grown and the structure was solved by X-ray diffraction (Supplementary Table S3). The crystallization conditions were based on prior studies of the parallel duplex formed by rA_{11} and used a fragment of poly(A) binding protein to promote crystallization (2). The protein acts to buffer the concentration of the oligonucleotide and does not incorporate into the crystals.

The structure of the duplex with a single deoxyribose sugar was very similar to that of the all RNA sequence (2). The asymmetric unit was composed of two strands forming ten adenine:adenine base pairs (Figure 4A). The 11th adenylate residue of each strand was base paired with an overhanging nucleotide on an adjacent strand. Due to the staggered strand alignment, the DNA nucleotides were offset so that two rA:dA base pairs were present. The adenine:adenine base pairs were stabilized by NH_4^+ cations that interact with the adenine N1 atoms and phosphate groups of the opposite strand (Figure 4B). The NH_4^+ bridge distances and angles with rA:dA base pairs were not affected by the deoxyribose sugar. Although the rA_5-dA-rA_5 crystals were grown at more acidic pH than the rA_{11} crystals (2), measurements of the C2-N1-C6 internal adenine ring angles suggest that the N1 atoms were unprotonated in the crystals. The deoxyribose sugar adopted an RNA-like 3′-*endo* sugar pucker as observed for the rA residues (Figure 4C).

The poly(A) duplex crystals are very densely packed with a solvent content of just 12.8%. This has the advantage of yielding very high resolution diffraction but also restricts the range of conformations within the crystal. It also raises the possibility that some features observed in the crystal structures arise from crystal packing or the selective crystallization of a subpopulation of poly(A) duplexes. To exam-

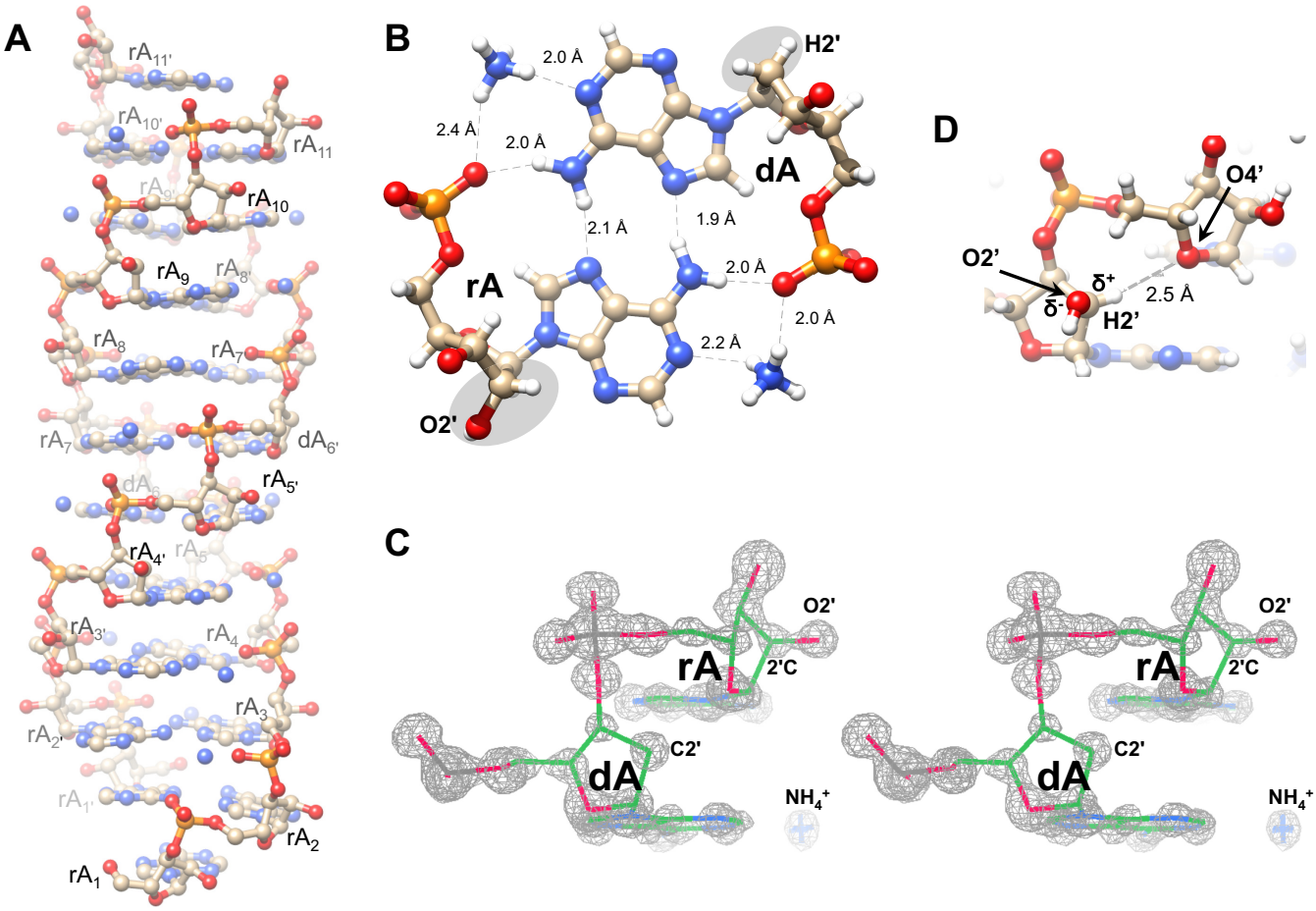

Figure 4. Crystal structure of the parallel duplex formed by rA_5-dA-rA_5. (**A**) Ball-and-stick representation of the duplex. (**B**) Hoogsteen hydrogen bonding of an adenine:adenine base pair and surrounding NH_4^+ ions. (**C**) Stereo view of dA-rA nucleotides in the F_OF_C omit map shows the C3'-*endo* sugar pucker of both sugars and bound NH_4^+ ions. The map was scaled at 5-fold above the noise; no negative density is visible. (**D**) Putative hydrogen between H2' and O4' that stabilizes the duplex. The O2' contributes to the electrostatic polarization of the H2' and increases the strength of the hydrogen bond.

ine the structure of the poly(A) duplexes in solution without crystal contacts, we turned to NMR spectroscopy.

NMR structure of a poly(A) duplex

We examined the duplexes formed by dT-rA_8 and related 9-mers with a single deoxyribose sugar. The NMR studies focused on the 2′-O-methylated oligomer, dT-mA_4-dA-mA_3, which offered the dual advantages of greater stability and the fortuitous resolution of the deoxyribose H2' and H2" signals. The two signals overlapped in the spectrum of dT-rA_4-dA-rA_3, which would have prevented determination of the sugar pucker of the dA residue.

One dimensional ^{1}H NMR spectra of dT-mA_4-dA-mA_3 acquired at pH 6 and 4 showed a downfield shift of the adenine NH_2 signals at pH 4, consistent with the formation of a parallel duplex (Figure 5A). The non-exchangeable proton resonances were assigned using intra-residue and sequential H1'(i)-H6/H8(i)-H1'(i-1) cross-peaks in the NOESY spectrum (Figure 5B and Supplementary Table S4). The amino (NH_2) protons were assigned using interstrand cross-peaks with H8 (i) and H3'(i-1) protons in the NOESY spectra in H_2O. These NOEs confirmed parallel duplex formation with hydrogen bonding between NH_2 protons and N7 (Figure 1). In addition, strong sequential H2 (i)-H1' (i+1) NOEs were detected. The thymine methyl showed a strong NOE to an adjacent adenine H2 and the thymine imino signal was shifted and narrowed due to stacking on the first adenine:adenine base pair. The DQF-COSY (Figure 5C), TOCSY and H,P-HSQC spectra (Supplementary Figure S7) were also used to assign sugar protons as well as phosphorus signals (Supplementary Table S4).

In agreement with the results from crystallography, the NMR analysis showed that the dA residue adopts a C3'-*endo* (North type) sugar pucker conformation, similar to the RNA residues. This was determined from the presence of strong H2"-H3' and H3'-H4' cross-peaks and very weak H1'-H2' cross-peaks in DQF-COSY spectra (Figure 5C). These indicate that the most populated conformation is North type. Sugar puckering was also determined from the sum of vicinal $J_{1'2'}$ and $J_{1'2"}$ couplings which equals 10.4 Hz for the dA6 nucleotides, corresponding to 10% S-type (C2'-*endo*) conformation: $\%S = (J_{1'2'} + J_{1'2"} - 9.8)/5.9$ (30). Strong intranucleotide H8-H3' and weak intra-nucleotide

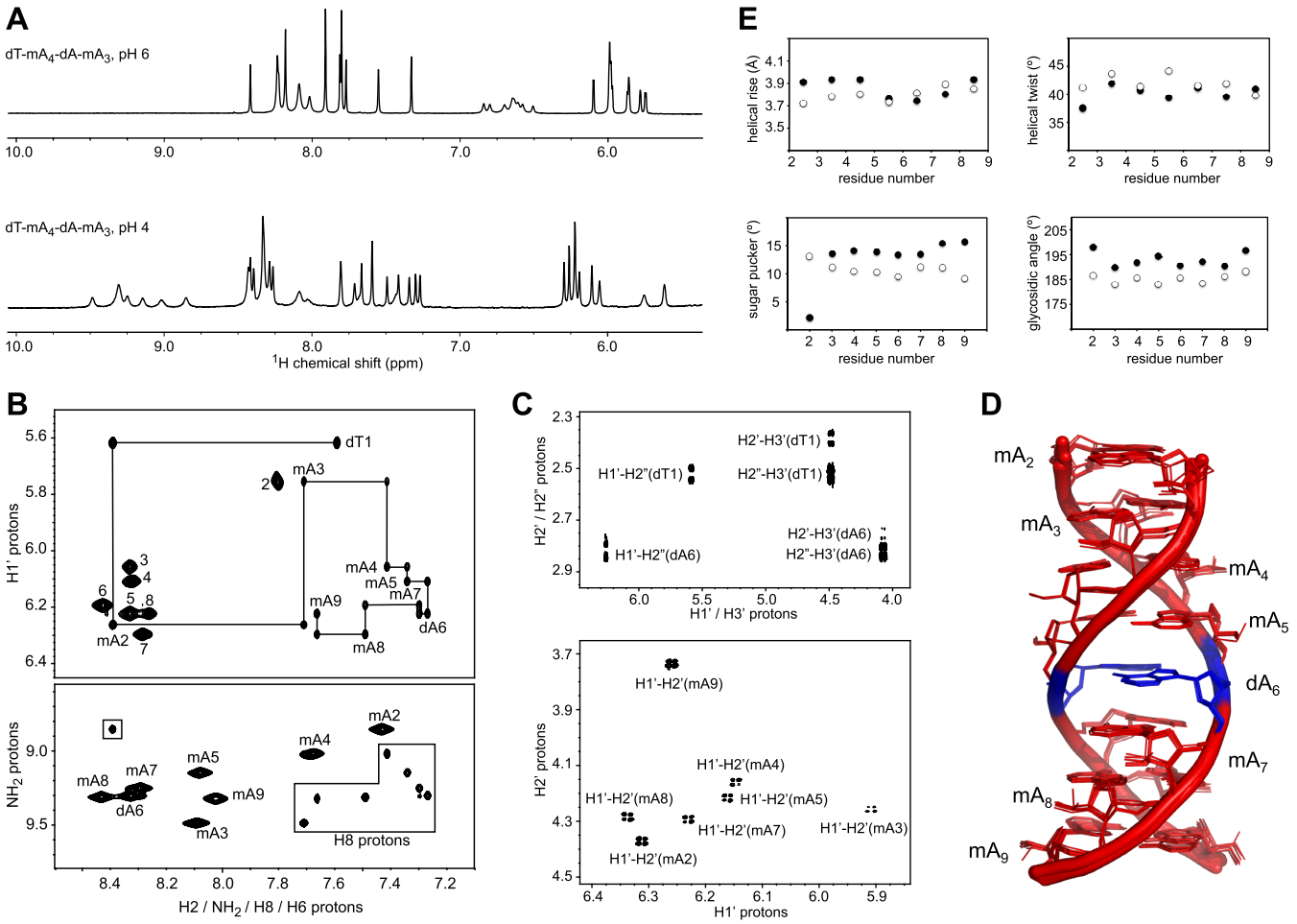

Figure 5. NMR solution structure of the dT-mA$_4$-dA-mA$_3$ parallel duplex. (**A**) NMR spectra of the single strand and duplex conformations at pH 6 and 4, respectively. Spectra were recorded at 10°C at 800 MHz. (**B**) NOESY spectrum (200 ms mixing time) confirms the parallel strand orientation. *Upper panel,* Sequential NOEs assignments, H1'(i)-H8(i)-H1'(i-1) (lines with peaks labeled by nucleotide name and number) and H2(i)-H1'(i+1) (labeled by nucleotide number), are shown. *Lower panel,* interstrand NH$_2$-H8 NOEs (boxed) confirm the parallel duplex structure. NOEs between the amino protons of adenine NH$_2$ group are labeled by nucleotide name and number. (**C**) COSY spectra confirm the 3′-*endo* confirmation of the ribose and deoxyribose sugars. The spectrum was recorded at 800 MHz in 100% D_2O buffer, pH 4, 10°C. (**D**) Superposition of ten converged structures of the mA$_4$-dA-mA$_3$ duplex. The 5′-terminal thymidylate is not shown; the deoxyadenylate residue is shown in blue. (**E**) Comparison of backbone parameters for poly(A) duplex in the dT-mA$_4$-dA-mA$_3$ solution structure (filled circles) and the rA$_{11}$ crystal structure (open circles, PDB ID: 4JRD).

H8-H2' NOEs were detected for all nucleotides in the duplex that is typical of a North-type sugar pucker.

In order to determine a duplex structure that is consistent with the experimental data, NMR-restrained molecular dynamic calculations were performed. The resulting NMR structure is the superposition of the ten best individual structures with an ensemble atomic RMSD of 0.29 Å (Figure 5D and Supplementary Table S5). Comparison of the average minimized structure of the mA$_4$-dA-mA$_3$ duplex with the 1 Å X-ray structure of the poly(A) duplex (PDB ID: 4JRD) resulted in an atomic RMSD of 0.53 Å for all the heavy atoms present. The helical rise of the mA$_4$-dA-mA$_3$ duplex is 3.7–3.9 Å, with a twist of 37–42°, a sugar pseudorotation phase angle of 2–16° corresponding to a C3'-*endo* pucker with glycosidic angles of 190–198° in the range of an anti-conformation (Figure 5E). All helical parameters are very similar to those reported for the 1 Å X-ray poly (rA) structure (2).

DISCUSSION

The conformational diversity of nucleic acid structures such as the i-motif, G-quartets, or triple helices makes them interesting materials for the design of molecular switches (31,32). In the case of poly(A) sequences, the regulation by pH and NH_4^+ ions of the parallel-stranded conformation opens up potential applications as pH sensors or ion-activated nanoswitches. The poly(A) duplex is also of interest due to its high stability relative to other parallel-stranded duplexes (7,8). The parallel poly(A) duplex has roughly double the melting temperature of Watson–Crick base-paired duplexes of the same length. This stability is due the electrostatic balance ('inner salt') of the negatively charged phosphates and the positive charges of the bases or bound cations (3).

For nanotechnology, chemical modification of the nucleotide sugar offers advantages in terms of ease of chemical synthesis, improved chemical stability and resistance to en-

zymatic degradation by nucleases. The C2' in the poly(A) duplex is an attractive position for modification as it is solvent-exposed on the exterior of the helix and not in a position to interact with other moieties. Surprisingly, we observed that the sugar composition strongly influences the stability of the poly(A) duplex. The incorporation of even a single deoxyribose or arabinose nucleoside strongly decreased the stability of duplexes in UV melting assays. Although duplex formation has been reported for poly(A) DNA oligomers (25), we were not able to observe duplexes in gel electrophoresis or spectroscopic assays. Our circular dichroism spectrum for dT-rA_8 matches the spectrum reported for dA_{15} (25) but we were not able to obtain the same spectrum with DNA (Figure 3B). NMR spectra at pH 4 of both dT-dA_8 and dT-dA_6 showed no shifts of amino resonances characteristic of base pairing and none of the NOEs expected for a parallel duplex (data not shown).

Analysis of the crystal and solution structures of poly(A) duplexes with deoxyribose sugars shows that the DNA nucleotides do not induce a significant distortion in the duplex. This suggests that the duplex sensitivity to C2' modifications arises from multiple, concurrent effects. Below, we discuss possible contributions to duplex stability from sugar pucker propensity, pKa shifts, hydrogen bonding and hydration.

Sugar pucker

The poly(A) duplex structures show that the sugars uniformly adopt a C3'-*endo* conformation (Figure 5E). The 2′-hydroxyl group in RNA favors a C3'-*endo* sugar pucker, so that the RNA oligomers are conformationally preorganized to form the poly(A) duplex. In the case of DNA, the sugar is more flexible and prefers the C2'-*endo* conformation (33). This entropic penalty may contribute to the destabilization by deoxyribose and also arabinose and 2′-deoxy-2′-fluoroarabinose, which prefer an O4'-*endo* sugar pucker (20,34). Studies of oligonucleotides containing 2′-deoxy-2′-fluororibose and 2′-O-methylribose have demonstrated that these modifications favor a C3'-*endo* pucker (35–37), which is consistent with the small change in stability we observed.

Shifts in the pKa of the adenine bases

We observed a shift in the pH optimum for the T_m for the rFA_{16} duplex, which suggests the 2′-fluoro modification decreases the pKa of the adenine bases. Measurements of adenine nucleotides have shown that 2′-fluoro (and 2′-O-methyl) substituents slightly decrease the basicity of the N1 atom relative to the ribonucleotide (38) but it is debatable if the size of the effect (∼0.1 pH units) is sufficient to explain the loss of stability observed. Cerutti and colleagues observed the increased thermal stability of the 2′-O-methylate duplex and attributed this to either a requirement for fewer protonated adenines or increased basicity of the adenine N1 atom of the 2′-O-methyladenosine residues (28). Interestingly, the 2′-fluoro and 2′-O-methyl modifications have contrasting effects on duplex stability when low pH and high NH_4^+ ion concentrations were compared. The 2′-fluoro modification was relatively destabilizing at low pH but clearly stabilized duplexes in 4.4 M NH_4Cl at pH 7. The 2′-O-methyl modification had a contrasting effect—relatively neutral in 4.4 M NH_4Cl but strongly stabilizing at low pH.

C2'-H···O4' hydrogen bonding

An additional destabilizing effect of DNA residues could be related to the loss of the electron withdrawing effect of the ribose 2′-OH. The hydroxyl group polarizes the geminal hydrogen that is positioned to interact with the O4' oxygen of an adjacent nucleotide (Figure 4D). In the crystal structure, all but one of C2'-H···O4' bond distances (2.4–2.6 Å) and angles (145°–173°) lie in the accepted range for an aliphatic hydrogen bond. Similarly polarization of the H2' atom by fluorine is consistent with the observed stability of poly(A) duplexes with 2′-deoxy-2′-fluoro-ribose. Such weak interactions have been invoked in other nucleic acid structures; for example, C1'-H···O4' contacts have been implicated as factor in i-motif stability (39) and FC-H2'···O interactions suggested to stabilize antiparallel helices with 2′-fluoro groups (40). The close C2'-H···O4' contact also explains why arabinose and 2′-deoxy-2′-fluoro-arabinose nucleotides are not tolerated. Epimerization of the 2′OH to generate arabinose would interfere with the positioning of the following nucleotide. Fluorine in the same position would generate the same steric clash.

Hydration and bound water

Enthalpic hydration of water molecules bridging hydrophilic groups is a well-established source of stabilization of nucleic acid structures. Studies comparing the stability and structure of RNA and DNA duplexes have shown that the higher stability of RNA and 2′-O-methyl-modified RNA is related to increased hydration (41,42). While differences in the numbers of bound waters around the dA residues were not observed in the crystal structure of rA_5-dA-rA_5, additional studies using molecular dynamics or NMR spectroscopy will likely show an important role of hydration in determining duplex stability.

Understanding the physical basis of duplex stability is important for developing the uses of parallel poly(A) duplexes for nanotechnology. Many possible applications of poly(A) duplexes as pH sensing switches can be imagined. Remarkably, we found that the introduction of C2' modifications affects duplex stability but does not alter the geometry of the duplex. The differential stability of the 2′-O-methyl and 2′-fluoro modifications offers the possibility of fine-tuning duplex formation to be selective to low pH or high NH_4^+ concentrations. Short 2′-O-methylated duplexes are remarkably stable at low pH and have many of the advantages of RNA as a building material. On the other hand, the significant stabilization (13°C) observed for 2′-fluoro-RNA in NH_4Cl suggests that it may be possible to design poly(A) duplexes with improved sensitivity to NH_4^+ ions.

ACCESSION NUMBERS

Atomic coordinates and structure factors for the rA_5-dA-rA_5 X-ray crystal structure have been deposited with the Protein Data bank under accession number 5VXQ. The

atomic coordinates of the dT-mA_4-dA-mA_3 NMR solution structure have been deposited under accession number 5TGG. The NMR chemical shifts have been deposited with the Biological Magnetic Resonance Bank under accession number 30184.

SUPPLEMENTARY DATA

Supplementary Data are available at NAR Online.

ACKNOWLEDGEMENTS

The authors are grateful to Dr Tara Sprules for recording proton NMR spectra at the Quebec-Eastern Canada High Field NMR Facility.

FUNDING

Natural Sciences and Engineering Research Council of Canada [299384-2011 to C.J.W.]; Canada Research Chair Program [950-213807 to C.J.W.]; Canadian Institutes of Health Research [MOP-14219 to K.G.]. Funding for open access charge: Natural Sciences and Engineering Research Council of Canada [299384-2011 to C.J.W.].
Conflict of interest statement. None declared.

REFERENCES

1. Guo,P. (2010) The emerging field of RNA nanotechnology. *Nat. Nanotechnol.*, **5**, 833–842.
2. Safaee,N., Noronha,A.M., Rodionov,D., Kozlov,G., Wilds,C.J., Sheldrick,G.M. and Gehring,K. (2013) Structure of the parallel duplex of poly(A) RNA: evaluation of a 50 year-old prediction. *Angew. Chem. Int. Ed. Engl.*, **52**, 10370–10373.
3. Rich,A., Davies,D.R., Crick,F.H. and Watson,J.D. (1961) The molecular structure of polyadenylic acid. *J. Mol. Biol.*, **3**, 71–86.
4. Leontis,N.B. and Westhof,E. (2001) Geometric nomenclature and classification of RNA base pairs. *RNA*, **7**, 499–512.
5. Gleghorn,M.L., Zhao,J., Turner,D.H. and Maquat,L.E. (2016) Crystal structure of a poly(rA) staggered zipper at acidic pH: evidence that adenine N1 protonation mediates parallel double helix formation. *Nucleic Acids Res.*, **44**, 8417–8424.
6. Acosta-Reyes,F.J., Alechaga,E., Subirana,J.A. and Campos,J.L. (2015) Structure of the DNA duplex d(ATTAAT)2 with Hoogsteen hydrogen bonds. *PLoS One*, **10**, e0120241.
7. Ramsing,N.B. and Jovin,T.M. (1988) Parallel stranded duplex DNA. *Nucleic Acids Res.*, **16**, 6659–6676.
8. van de Sande,J.H., Ramsing,N.B., Germann,M.W., Elhorst,W., Kalisch,B.W., von Kitzing,E., Pon,R.T., Clegg,R.C. and Jovin,T.M. (1988) Parallel stranded DNA. *Science*, **241**, 551–557.
9. Rippe,K., Fritsch,V., Westhof,E. and Jovin,T.M. (1992) Alternating d(G-A) sequences form a parallel-stranded DNA homoduplex. *EMBO J*, **11**, 3777–3786.
10. Gehring,K., Leroy,J.L. and Gueron,M. (1993) A tetrameric DNA structure with protonated cytosine.cytosine base pairs. *Nature*, **363**, 561–565.
11. Ingale,S.A., Leonard,P., Tran,Q.N. and Seela,F. (2015) Duplex DNA and DNA-RNA hybrids with parallel strand orientation: 2′-deoxy-2′-fluoroisocytidine, 2′-deoxy-2′-fluoroisoguanosine, and canonical nucleosides with 2′-fluoro substituents cause unexpected changes on the double helix stability. *J. Org. Chem.*, **80**, 3124–3138.
12. Burnett,J.C. and Rossi,J.J. (2012) RNA-based therapeutics: current progress and future prospects. *Chem. Biol.*, **19**, 60–71.
13. Deleavey,G.F. and Damha,M.J. (2012) Designing chemically modified oligonucleotides for targeted gene silencing. *Chem. Biol.*, **19**, 937–954.
14. Collin,D. and Gehring,K. (1998) Stability of chimeric DNA/RNA cytosine tetrads: implications fori-Motif formation by RNA. *J. Am. Chem. Soc.*, **120**, 4069–4072.
15. Assi,H.A., Harkness,R.W.t., Martin-Pintado,N., Wilds,C.J., Campos-Olivas,R., Mittermaier,A.K., Gonzalez,C. and Damha,M.J. (2016) Stabilization of i-motif structures by 2′-beta-fluorination of DNA. *Nucleic Acids Res.*, **44**, 4998–5009.
16. Damha,M.J. and Ogilvie,K.K. (1993) Oligoribonucleotide synthesis. The silyl-phosphoramidite method. *Methods Mol. Biol.*, **20**, 81–114.
17. Puglisi,J.D. and Tinoco,I. Jr (1989) Absorbance melting curves of RNA. *Methods Enzymol.*, **180**, 304–325.
18. Delaglio,F., Grzesiek,S., Vuister,G.W., Zhu,G., Pfeifer,J. and Bax,A. (1995) NMRPipe: a multidimensional spectral processing system based on UNIX pipes. *J. Biomol. NMR*, **6**, 277–293.
19. Johnson,B.A. and Blevins,R.A. (1994) NMR View: a computer program for the visualization and analysis of NMR data. *J. Biomol. NMR*, **4**, 603–614.
20. Denisov,A.Y., Noronha,A.M., Wilds,C.J., Trempe,J.F., Pon,R.T., Gehring,K. and Damha,M.J. (2001) Solution structure of an arabinonucleic acid (ANA)/RNA duplex in a chimeric hairpin: comparison with 2′-fluoro-ANA/RNA and DNA/RNA hybrids. *Nucleic Acids Res.*, **29**, 4284–4293.
21. Kim,S.G., Lin,L.J. and Reid,B.R. (1992) Determination of nucleic acid backbone conformation by 1H NMR. *Biochemistry*, **31**, 3564–3574.
22. Brunger,A.T., Adams,P.D., Clore,G.M., DeLano,W.L., Gros,P., Grosse-Kunstleve,R.W., Jiang,J.S., Kuszewski,J., Nilges,M., Pannu,N.S. *et al.* (1998) Crystallography & NMR system: a new software suite for macromolecular structure determination. *Acta Crystallogr. D Biol. Crystallogr.*, **54**, 905–921.
23. Lu,X.J. and Olson,W.K. (2003) 3DNA: a software package for the analysis, rebuilding and visualization of three-dimensional nucleic acid structures. *Nucleic Acids Res.*, **31**, 5108–5121.
24. Lu,X.J. and Olson,W.K. (2008) 3DNA: a versatile, integrated software system for the analysis, rebuilding and visualization of three-dimensional nucleic-acid structures. *Nat. Protoc.*, **3**, 1213–1227.
25. Chakraborty,S., Sharma,S., Maiti,P.K. and Krishnan,Y. (2009) The poly dA helix: a new structural motif for high performance DNA-based molecular switches. *Nucleic Acids Res.*, **37**, 2810–2817.
26. Leng,M. and Felsenfeld,G. (1966) A study of polyadenylic acid at neutral pH. *J. Mol. Biol.*, **15**, 455–466.
27. Kool,E.T. (1997) Preorganization of DNA: design principles for improving nucleic acid recognition by synthetic oligonucleotides. *Chem. Rev.*, **97**, 1473–1488.
28. Bobst,A.M., Rottman,F. and Cerutti,P.A. (1969) Effect of the methylation of the 2′-hydroxyl groups in polyadenylic acid on its structure in weakly acidic and neutral solutions and on its capability to form ordered complexes with polyuridylic acid. *J. Mol. Biol.*, **46**, 221–234.
29. Patra,A., Paolillo,M., Charisse,K., Manoharan,M., Rozners,E. and Egli,M. (2012) 2′-Fluoro RNA shows increased Watson-Crick H-bonding strength and stacking relative to RNA: evidence from NMR and thermodynamic data. *Angew. Chem. Int. Ed. Engl.*, **51**, 11863–11866.
30. Rinkel,L.J. and Altona,C. (1987) Conformational analysis of the deoxyribofuranose ring in DNA by means of sums of proton-proton coupling constants: a graphical method. *J. Biomol. Struct. Dyn.*, **4**, 621–649.
31. Idili,A., Ricci,F. and Vallee-Belisle,A. (2017) Determining the folding and binding free energy of DNA-based nanodevices and nanoswitches using urea titration curves. *Nucleic Acids Res.*, **45**, 7571–7580.
32. Peng,P., Shi,L., Wang,H. and Li,T. (2017) A DNA nanoswitch-controlled reversible nanosensor. *Nucleic Acids Res.*, **45**, 541–546.
33. Saenger,W. (1984) *Principles of Nucleic Acids Structure*. Springer, NY.
34. Trempe,J.F., Wilds,C.J., Denisov,A.Y., Pon,R.T., Damha,M.J. and Gehring,K. (2001) NMR solution structure of an oligonucleotide hairpin with a 2′F-ANA/RNA stem: implications for RNase H specificity toward DNA/RNA hybrid duplexes. *J. Am. Chem. Soc.*, **123**, 4896–4903.
35. Ikeda,H., Fernandez,R., Wilk,A., Barchi,J.J. Jr, Huang,X. and Marquez,V.E. (1998) The effect of two antipodal fluorine-induced sugar puckers on the conformation and stability of the Dickerson-Drew dodecamer duplex [d(CGCGAATTCGCG)]2. *Nucleic Acids Res.*, **26**, 2237–2244.

36. Kawasaki,A.M., Casper,M.D., Freier,S.M., Lesnik,E.A., Zounes,M.C., Cummins,L.L., Gonzalez,C. and Cook,P.D. (1993) Uniformly modified 2′-deoxy-2′-fluoro-phosphorothioate oligonucleotides as nuclease-resistant antisense compounds with high affinity and specificity for RNA targets. *J. Med. Chem.*, **36**, 831–841.
37. Lesnik,E.A., Guinosso,C.J., Kawasaki,A.M., Sasmor,H., Zounes,M., Cummins,L.L., Ecker,D.J., Cook,P.D. and Freier,S.M. (1993) Oligodeoxynucleotides containing 2′-O-modified adenosine: synthesis and effects on stability of DNA:RNA duplexes. *Biochemistry*, **32**, 7832–7838.
38. Chatterjee,S., Pathmasiri,W., Plashkevych,O., Honcharenko,D., Varghese,O.P., Maiti,M. and Chattopadhyaya,J. (2006) The chemical nature of the 2′-substituent in the pentose-sugar dictates the pseudoaromatic character of the nucleobase (pKa) in DNA/RNA. *Org. Biomol. Chem.*, **4**, 1675–1686.
39. Berger,I., Egli,M. and Rich,A. (1996) Inter-strand C-H…O hydrogen bonds stabilizing four-stranded intercalated molecules: stereoelectronic effects of O4′ in cytosine-rich DNA. *Proc. Natl. Acad. Sci. U.S.A.*, **93**, 12116–12121.
40. Martin-Pintado,N., Deleavey,G.F., Portella,G., Campos-Olivas,R., Orozco,M., Damha,M.J. and Gonzalez,C. (2013) Backbone FC-H…O hydrogen bonds in 2′F-substituted nucleic acids. *Angew. Chem. Int. Ed. Engl.*, **52**, 12065–12068.
41. Egli,M., Portmann,S. and Usman,N. (1996) RNA hydration: a detailed look. *Biochemistry*, **35**, 8489–8494.
42. Auffinger,P. and Westhof,E. (2001) Hydrophobic groups stabilize the hydration shell of 2′-O-methylated RNA duplexes. *Angew. Chem. Int. Ed. Engl.*, **40**, 4648–4650.